Received 2016 March 21; accepted 2016 May 3; published 2016 July 18
Preprint typeset using LaTeX style emulateapj v. 5/2/11

arXiv:1605.01284v2 [astro-ph.GA] 3 Aug 2016

EXPANDING MOLECULAR BUBBLE SURROUNDING TYCHO'S SUPERNOVA REMNANT (SN 1572) OBSERVED WITH THE IRAM 30 M TELESCOPE: EVIDENCE FOR A SINGLE-DEGENERATE PROGENITOR

Ping Zhou (周平) [1,2], Yang Chen (陳陽) [1,2], Zhi-Yu Zhang (張智昱)[3,4], Xiang-Dong Li (李向東)[1,2], Samar Safi-Harb[5], Xin Zhou (周鑫)[6], and Xiao Zhang (張瀟)[1]

Received 2016 March 21; accepted 2016 May 3; published 2016 July 18

ABSTRACT

Whether the progenitors of SNe Ia are single-degenerate or double-degenerate white dwarf (WD) systems is a highly debated topic. To address the origin of the Type Ia Tycho's supernova remnant (SNR), SN 1572, we have carried out a ^{12}CO J=2–1 mapping and a 3-mm line survey toward the remnant using the IRAM 30 m telescope. We show that Tycho is surrounded by a clumpy molecular bubble at a local standard of rest velocity of ~ 61 km s^{-1} which expands at a speed of ~ 4.5 km s^{-1} and has a mass of ~ 220 $M_{\odot}$ (at the distance of 2.5 kpc). Enhanced ^{12}CO J=2–1 line emission relative to ^{12}CO J=1–0 emission and possible line broadenings (in velocity range -64 to -60 km s^{-1}) are found at the northeastern boundary of the SNR, where the shell is deformed and decelerated. These features, combined with the morphological correspondence between the expanding molecular bubble and Tycho, suggest that the SNR is associated with the bubble at the velocity range -66 to -57 km s^{-1}. The most plausible origin for the expanding bubble is the fast outflow (with velocity of hundreds km s^{-1}) driven from the vicinity of a WD as it accreted matter from a nondegenerate companion star. The SNR has been expanding in the low-density wind-blown bubble, and the shock wave has just reached the molecular cavity wall. This is the first unambiguous detection of an expanding bubble driven by the progenitor of a Type-Ia SNR, which constitutes evidence for a single-degenerate progenitor for this SN Ia.

Subject headings: binaries: close — ISM: individual objects (Tycho's supernova remnant; SN 1572; G120.1+1.4) — ISM: supernova remnants

1. INTRODUCTION

Type Ia supernovae (SNe Ia) are catastrophic thermonuclear explosions of massive carbon/oxygen white dwarfs (WDs) with mass exceeding a critical value. Due to the low intrinsic scatter at the peak luminosity, SNe Ia have been employed as "standard candles" for measuring distances and determining cosmological parameters (Riess et al. 1998; Perlmutter et al. 1999). The single-degenerate (SD) and double-degenerate (DD) models are the most popular scenarios for the SN Ia progenitors. The SD models assume a WD in a close binary system accreting material from a nondegenerate companion (Whelan & Iben, 1973), while the DD models involve a merger of two WDs (Webbink, 1984).

The historical supernova remnant (SNR) Tycho (or SN 1572, G120.1+1.4) is thought to originate from an SN Ia as evidenced by its light curve (Baade 1945; Ruiz-Lapuente 2004), X-ray spectroscopic analysis (Badenes et al. 2006), and light echo spectrum (Krause et al. 2008). However, there is no consensus on its progenitor system. The SD scenario is supported by the discovery of a fast-moving, type G0–G2 subgiant (Tycho-G) in the SNR center, which was suggested to be the surviving companion of the SN (Ruiz-Lapuente et al. 2004). Lu et al. (2011) found an X-ray arc inside Tycho, which was probably produced by the interaction between the SN ejecta and the companion star's envelope lost due to the impact of the explosion. The SD scenario has, however, been questioned (Badenes et al. 2007). While there is a dispute over whether Tycho-G is the ex-companion (see Xue & Schaefer 2015 and references therein), other candidates such as Tycho-B (Kerzendorf et al. 2013) and Tycho-E (Ihara et al. 2007) were also proposed. Another independent method is needed to resolve the progenitor problem of Tycho.

One key aspect of the SD and DD scenarios is the presence or absence, respectively, of outflows from the binary system during the pre-SN evolution (Badenes et al. 2007). According to the SD scenario, a strong wind is driven to stabilize the mass transfer when the mass accretion rate exceeds a certain critical value (e.g., Hachisu et al. 1996; Li & van den Heuvel 1997; Hachisu et al. 1999). The strong wind could blow a low-density bubble before the SN explodes and the shock wave interacts with the dense material of the wind cavity (e.g, RCW 86; Vink et al. 1997; Broersen et al. 2014). The size of the wind-blown bubble (WBB) depends not only on the wind parameters, but also the on the density of the ambient medium (e.g., Weaver et al. 1977; Koo & Mckee 1992a, 1992b).

Tycho is is proably the only known Type Ia SNR interacting with a molecular cloud (MC). Radio observa-

[1] Department of Astronomy, Nanjing University, Nanjing 210023, China; pingzhou@nju.edu.cn
[2] Key Laboratory of Modern Astronomy and Astrophysics, Nanjing University, Ministry of Education, China
[3] Institute for Astronomy, University of Edinburgh, Royal Observatory, Blackford Hill, Edinburgh EH9 3HJ, UK
[4] ESO, Karl Schwarzschild Strasse 2, D-85748 Garching, Munich, Germany
[5] Department of Physics and Astronomy, University of Manitoba, Winnipeg, MB R3T 2N2, Canada
[6] Purple Mountain Observatory, CAS, 2 West Beijing Road, Nanjing 210008, China

TABLE 1
CO observations of Tycho with the IRAM 30 m telescope

Lines	Position	Map Size	HPBW	$N(H_2)$ 10^{20} cm^{-2}	Azimuth Angle[a]
^{12}CO J=2–1	($00^h25^m21^s.0$, 64°08′35″.0)	12′ × 12′	11″	-	-
^{12}CO ^{13}CO J=1–0	P1($00^h25^m53^s.1$, 64°08′24″.8)	-	21″	7.3	87°
^{12}CO ^{13}CO J=1–0	P2($00^h25^m51^s.7$, 64°08′55″.8)	-	21″	5.2	79°
^{12}CO ^{13}CO J=1–0	P3($00^h25^m50^s.5$, 64°09′23″.0)	-	21″	7.7	71°
^{12}CO ^{13}CO J=1–0	P4($00^h25^m56^s.0$, 64°08′46″.8)	-	21″	9.3	82°
^{12}CO ^{13}CO J=1–0	P5($00^h25^m48^s.8$, 64°09′51″.0)	-	21″	7.3	62°
^{12}CO ^{13}CO J=1–0	P6($00^h25^m54^s.9$, 64°09′17″.0)	-	21″	8.6	75°

[a] The azimuth angle of P1-6 (counterclockwise from the north). The geometric center ($00^h25^m19^s.4$, 64°08′13″.98, J2000) determined by Warren et al. (2005) is used here.

tions spanning a 10 yr interval revealed slow expansion in the northeast, where the shell is encountering denser material (Reynoso et al. 1997, 1999). Lee et al. (2004) found that the SNR is likely surrounded by a molecular shell at $V_{\rm LSR} \sim -67$ to -60 km s^{-1} with the Nobeyama ^{12}CO J=1–0 observation (beam width of 16″). The MC in this velocity interval has also been studied in ^{12}CO J=1–0 lines (beam width of 60″; Cai et al. 2009), and in ^{12}CO J=2–1 and J=3–2 lines (beam width of 130″ and 80″, respectively; Xu et al. 2011). Shock interaction with the adjacent dense gas provides a reasonable mechanism for the hadronic γ-ray emission arising from Tycho (Zhang et al. 2013). The association of the MC with Tycho has not been confirmed yet and still requires kinematic evidence such as line broadening and a large high-to-low excitation line ratio (see Jiang et al. 2010 for observational evidence for judging the contact of SNRs with MCs).

To confirm or refute the SNR–MC association and to address the progenitor of Tycho, we have performed high-resolution CO observations with the IRAM 30 m telescope.

2. OBSERVATION

We have performed observations of molecular lines toward Tycho in 2013 August with the IRAM 30 m telescope. The ^{12}CO J=2–1 (at 230.538 GHz) mapping was conducted with the on-the-fly position switching mode using the 9-pixel dual-polarization heterodyne receiver array (HERA) and the fast Fourier transform spectrometer (FTS). The backend FTS provides a bandwidth of 0.5 GHz and a velocity resolution of 0.063 km s^{-1}. The ^{12}CO J=2–1 observation covered a 12′ × 12′ region centered at ($00^h25^m21^s$, 64°08′35″, J2000), with an antenna half-power beam width (HPBW) of 10″.7. The data were then converted to a cube with a spatial pixel size of 5″.3. After correcting the main-beam efficiency of 59% at 230.5 GHz, the mean rms noise level of the main-beam temperature ($T_{\rm mb}$) is 0.32 K in each pixel with a velocity resolution of 0.5 km s^{-1}.

We carried out a line survey at the 3 mm band at six positions (labeled with plus signs in the bottom-right panel of Figure 1) with the Eight Mixer Receiver (EMIR) of the IRAM 30 m telescope. The backend FTS provided a 16-GHz frequency coverage in 92–100 GHz and 108–115 GHz. The velocity resolution, angular resolution, and main beam efficiency were about 0.5 km s^{-1}, 21″, and 78%, respectively. The mean rms noise levels of $T_{\rm mb}$ are 0.06–0.10 K at 115 GHz and 0.02–0.05 K at 110 GHz. The information of the observed lines is summarized in Table 1.

In addition, we retrieved the public archival ^{13}CO J=1–0 mapping data taken during 2004 May and June with the 13.7 m millimeter-wavelength telescope of the Purple Mountain Observatory (PMO) at Delingha in China. The data with a velocity resolution of 0.11 km s^{-1} were convolved to an angular resolution of 2′ (initial HPBW was 1′) to match the grid spacing of 2′. We used the CLASS package of GILDAS to reduce the data and the KARMA (Gooch 1996) and IDL software packages for the data analysis and visualization.

3. RESULTS

The field of Tycho shows emission of ^{12}CO J=2–1 in the LSR velocity range of -67 to -56 km s^{-1} (see Figure 1). The overall emission has two peaks around the $V_{\rm LSR} = -65$ km s^{-1} and -62 km s^{-1}, with a few weak structures at the velocity range -58 to -54 km s^{-1}. The molecular gas near Tycho is highly clumpy, as revealed in the channel maps. The ^{12}CO J=2–1 emission has a $T_{\rm mb} \lesssim 3$ K in most of the field, which is lower than the kinetic temperature of typical interstellar MC ($\sim$ 10 K). The low main-beam temperature further supports the MC being highly clumpy (size $<$ 0.14 pc at an assumed distance of 2.5 kpc) and not resolved in our observation. The brightest ^{12}CO J=2–1 emission ($T_{\rm mb}$(peak) = 7.3 K) arises from the southwestern end of a molecular strip ($00^h25^m56^s.96$, 64°08′56″.77, J2000), which in projection contacts the eastern concave of the radio shell (see Figure 1). At $V_{\rm LSR} = -62.6$ km s^{-1}, the relatively bright ^{12}CO J=2–1 clumps are generally distributed surrounding the shell of the SNR and display similar morphology to that previously shown in the ^{12}CO J=1–0 emission (Lee et al. 2004). The clumps contacting the SNR in the east, southeast, and north are consistent with the locations showing low expansion rate from the radio observations (Reynoso et al. 1997).

In order to search for kinematic evidence of the SNR–MC interaction, we investigate the profiles of multiple molecular lines. Only ^{12}CO J=1–0 (115.271 GHz) and ^{13}CO J=1–0 (110.201 GHz) lines were detected in the 3 mm band line survey toward the six positions at the northeastern boundary of Tycho. Figure 2 shows the ^{12}CO J=1–0, ^{13}CO J=1–0, and ^{12}CO J=2–1 lines at the six positions. Here the ^{12}CO J=2–1 data were convolved to 21″.3 to match the beam size of ^{12}CO J=1–0 data. We searched for broad ^{12}CO line profiles in order

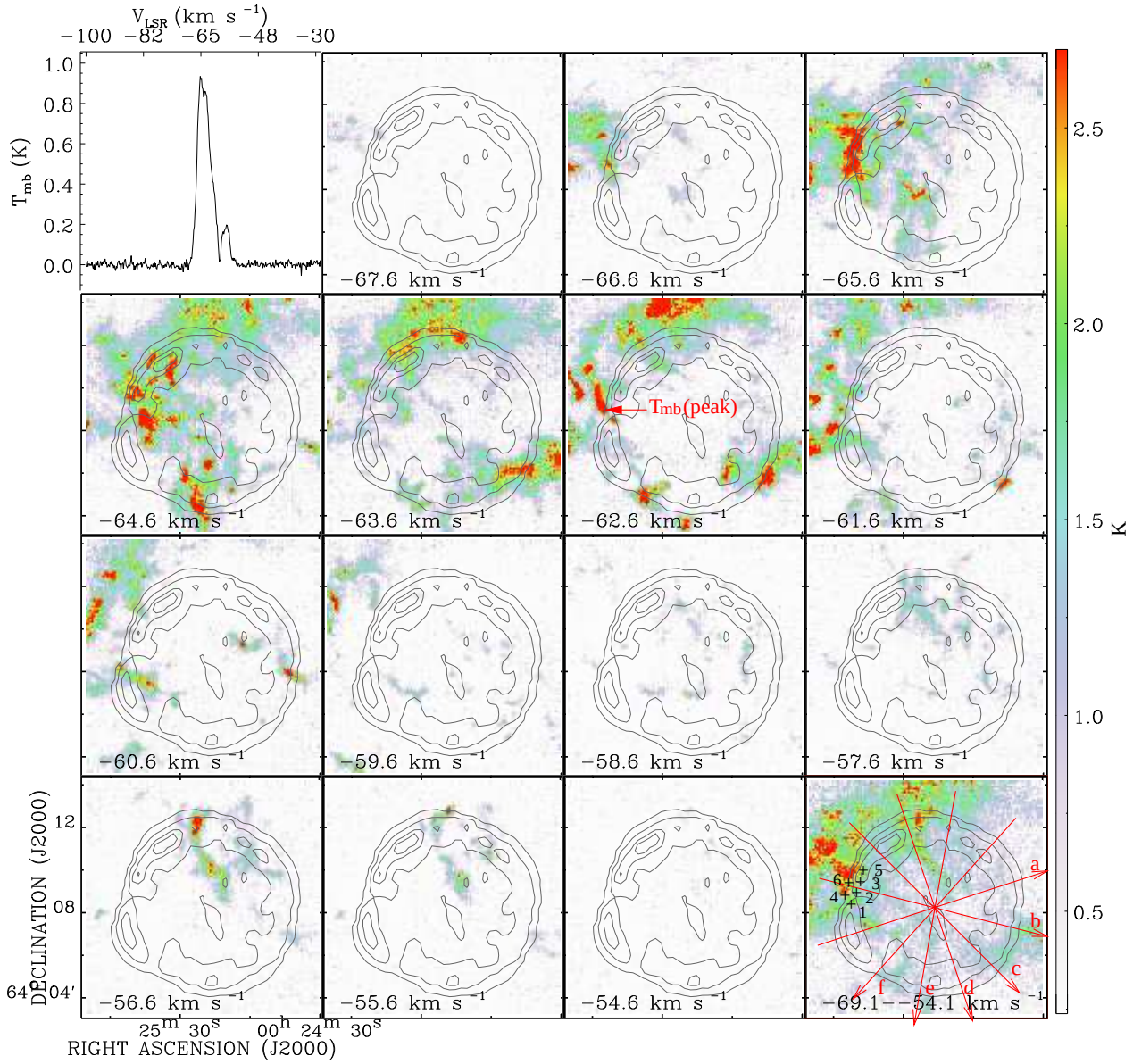

FIG. 1.— The upper-left panel shows the average spectrum of ^{12}CO J=2–1 in the field of view. The bottom-right panel shows the velocity-integrated intensity in the velocity range −68.1−−54.1 km s^{-1} with the maximum intensity scale of 13.5 K. The six plus signs label the positions where the 3-mm line survey observations were made. The data used in the position-velocity diagrams (in Figure 3) are selected along the red lines. Other panels reveal the ^{12}CO J=2–1 intensity channel maps with a step of 1 km s^{-1}, overlaid with contours of the 1.4 GHz continuum of the NRAO VLA Sky Survey. The color bar shows the intensity scale of the channel maps.

to trace the kinematic structure of the shocked molecular gas, and high temperature of ^{12}CO J=2–1 to trace heated gas. At the positions "P2" and "P3", we find ^{12}CO line wings at $\sim$ 63 km s^{-1} where ^{13}CO emission was not detected. Such high ^{12}CO/^{13}CO ratios suggest that the ^{12}CO lines are optically thin due to low CO column density or/and large velocity gradient, as commonly seen in the line broadenings from the shocked clouds. At position "P2", the ^{12}CO J=2–1 emission in the velocity range −64 to −60 km s^{-1} is stronger than ^{12}CO J=1–0, with a velocity-integrated intensity ratio of $\sim$ 1.6. Such a large high-to-low excitation line ratio needs high-excitation conditions and is generally regarded as evidence of shock heating and perturbation (Seta et al. 1998; Chen et al. 2014). The azimuth angle of "P2" (79°; counterclockwise from the north) is consistent with the angle where the forward shocks are significantly decelerated during 2003-2007 (see Fig. 5 in Katsuda et al. 2010).

An expanding bubble is revealed in the position-velocity diagrams of ^{12}CO J=2–1 across the center of Tycho (see Figure 3). The diagrams are obtained from six cuts starting from the position angle (PA) of 287° and with a 30° decrement (labeled with "a"−"f" in the bottom right panel of Figure 1). The morphology of the molecular gas revealed in the position-velocity dimen-

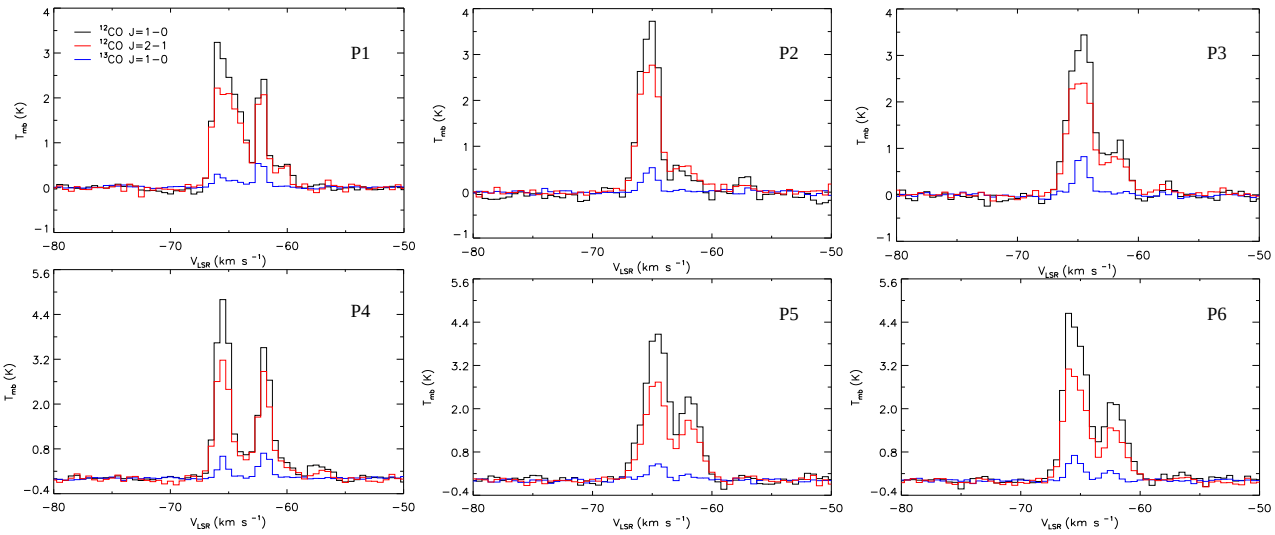

FIG. 2.— Spectra of CO and its isotope in six positions at the northeastern boundary of Tycho (see Figure 1 and Table 1).

sions is very similar to an expanding sphere centered at ~ 61 km s^{-1} with an angular size of $\sim 8'$ and a velocity of ~ 4.5 km s^{-1}. Most of the gas is at the blue-shifted side ($V_{\rm LSR} = -66$ to -60 km s^{-1}). The consistency of the size and position of the expanding circular gas with those of Tycho, together with the cavity morphology (see Figure 1) and large ^{12}CO J=2–1-to-J=1–0 ratio at $V_{\rm LSR} \sim -64$ to -60 km s^{-1} (see Figure 2), implies that Tycho is associated with the expanding molecular bubble at $V_{\rm LSR} = -66$ to -57 km s^{-1}.

4. DISCUSSION

4.1. *Properties of the MC surrounding Tycho*

Using the IRAM 30 m observations, we show that Tycho is evolving in an expanding molecular bubble at $V_{\rm LSR} \sim 61$ km s^{-1}. The shock of the SNR might not have extensively impacted the molecular gas, but only contacted partially, e.g., in the northeast where the rim is deformed and decelerated as revealed in radio (Reynoso et al. 1997) and X-ray observations (Katsuda et al. 2010). Although the data do not show very broad CO lines even with the best angular resolution in CO observations obtained to date (10.″7), the large ^{12}CO J=2–1-to-J=1–0 ratio and ^{12}CO-to-^{13}CO ratios are present in the northeast of the remnant. This can be interpreted as the shocked clumps remaining unresolved with current observations (low brightness temperature; see Section 3), and the shock front having just reached the molecular medium in the recent past (within a few tens of years; Reynoso et al. 1999) and swept up a small amount of gas.

This molecular gas can be the dense target of collision by the cosmic-ray protons accelerated by Tycho's blast shock, which gives rise to γ-ray emission due to hadronic interaction. A high ambient gas density provides a possibility of the relatively low fraction of energy deposited to the shock-accelerated protons in the young Tycho SNR (Zhang et al. 2013).

The suggested distance of Tycho varies between 1.7 and 5 kpc according to different methods (Albinson et al. 1986; Schwarz et al. 1995; Krause et al. 2008; Hayato et al. 2010). As suggested in Zhang et al. (2013; see also Lee et al. 2004), the system velocity of -62 km s^{-1} of the MC allows the alternative distances of 4.0 and 2.5 kpc, and the absence of an HI absorption feature at -46 to -41 km s^{-1} (Tian & Leahy 2011) is suggestive of the nearer distance. Hence, we adopt a distance of ~ 2.5 kpc for Tycho.

The column density of the molecular gas at the six positions at the northeastern boundary of the SNR is estimated with the ^{13}CO line detected at $V_{\rm LSR} = -67$ to -60 km s^{-1}. Assuming that the rotational levels of the ^{13}CO molecules are in local thermodynamic equilibrium and the ^{13}CO lines are optically thin, we obtain a column density of H_2 $N(H_2) = 1.21 \times 10^{20} \int T_{\rm mb,13CO}(v)dv[1 - \exp(-5.29/T_{\rm ex})]^{-1}$ cm^{-2}, where the relative abundance ratio of H_2 to ^{13}CO is taken as 5×10^5 (Dickman 1978). A typical temperature of 10 K in MCs is adopted here for the excitation temperature $T_{\rm ex}$. The $N(H_2)$ values at the six positions at the northeastern boundary of the Tycho are derived to be in the range (5.2–9.3) $\times 10^{20}$ cm^{-2} as tabulated in Table 1.

We use the PMO ^{13}CO J=1–0 line mapping to estimate the mass of the MC surrounding the SNR. The ^{13}CO emission is selected in a circular region with a radius of 6′ and centered at point ($00^{\rm h}25^{\rm m}19^{\rm s}.4$, $64°08'13''.98$, J2000). The region encloses bright ^{12}CO J=2–1 emission present in Figure 1. The mean $N(H_2)$ in the region is $\sim 1.6 \times 10^{20}$ cm^{-2} and the mass of the MC is $\sim 220\ d_{2.5}^2\ M_\odot$, where $d_{2.5}$ is the distance in units of 2.5 kpc. This mass is one order of magnitude lower than that derived with ^{12}CO lines and the CO-to-H_2 conversion factor (Cai et al. 2009). The standard conversion factor is a rough estimate of the global mass of a giant MC with a mass of 10^4–10^6 $M_\odot$ (Dame et al. 2001), and has a large variability on small spatial scales (Bolatto et al. 2013).

4.2. *Expanding molecular bubble as an implication for a SD progenitor*

The bubble surrounding Tycho has an inner radius of about 4′ (corresponding to 3 $d_{2.5}$ pc) and a mass of $\sim 220\ d_{2.5}^2\ M_\odot$. Such an expanding bubble could be a WBB created with a central star/system, while the shock wave

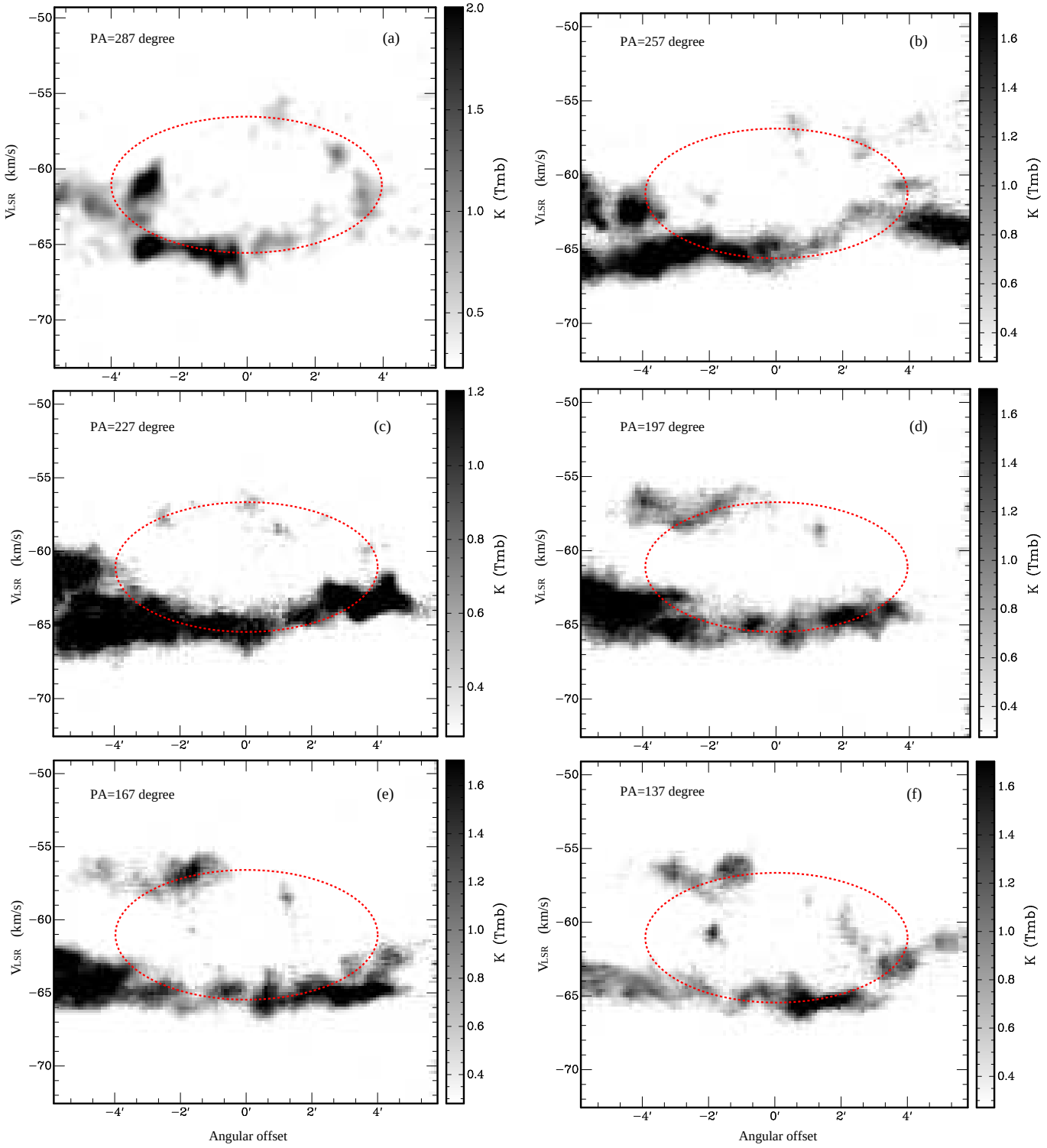

FIG. 3.— Position-velocity diagrams of ^{12}CO J=2–1 emission across the SNRs along six cuts (equivalent to optical long-slit spectra; the directions of the cuts with a 30° decrement are displayed in the bottom-right panel of Figure 1). Panel a: the diagram is obtained along the 10.′′7-wide cut "a" with PA= 287° and the data are smoothed with a Gaussian kernel of (16′′, 0.6 km s^{-1}). Panel b–f: the diagrams are for 2′-wide cuts "b"–"f". The data with signal-to-noise ratio $\geq$ 3 are displayed. The dashed ellipses indicate the sphere centered at ($00^{h}25^{m}20^{s}$, 64°08′14′′, 61 km s^{-1}), with a radius of 4′, and expanding with a velocity of 4.5 km s^{-1}.

of the SNR is not a plausible source since the shock wave has just reached the boundary of the molecular cavity and the velocity width (FWHM) of the CO lines in the field is smaller than the expanding velocity of 5 km s^{-1}.

First, we can exclude a massive star as the central source. If the molecular bubble here was created by a massive star, using the linear relationship between the maximum WBB sizes of main-sequence OB stars in the molecular environment $R_{\rm m}$ and the initial masses of the

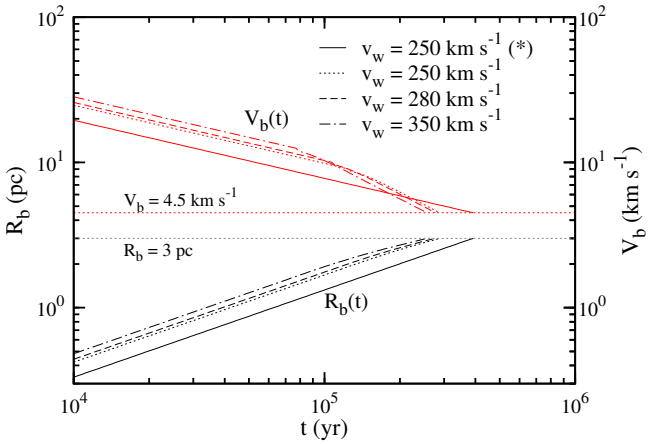

FIG. 4.— Exemplified possible evolutionary paths of the wind bubble with various sets of parameters. Paths A–D (with parameters tabulated in Table 2) are plotted with solid, dotted, dashed, and dot-dashed lines, respectively. The star sign indicates the evolution path that the wind lasts until the SN explosion (path A).

stars M (Chen et al. 2013): $p_5^{1/3} R_{\rm m}({\rm pc}) \approx 1.22 M/M_\odot - 9.16$, where p_5 is the interclump pressure p/k scaled to 10^5 cm^{-3} K ($p_5 \sim 1$ in the interclump medium of MCs; Chevalier 1999; Blitz 1993; Krumholz et al. 2009), the mass of the star would be $\gtrsim 10\ M_\odot$ (B2 type or earlier). Such massive early-type stars have not been detected inside the bubble.

The alternative explanation is related to the progenitor system of Tycho. Substantial outflow with a mass-loss rate $\dot{M} \sim 10^{-6}\ M_\odot\,{\rm yr}^{-1}$ has been suggested to occur when a carbon/oxygen WD accretes matter from a main-sequence or (slightly) evolved companion star. The wind may have a velocity $v_{\rm w}$ larger than a few hundred km s^{-1}(Kato & Hachisu 1999).

The fast wind from the accretion disk can evacuate a low-density cavity in which radiative losses are not important (Badenes et al. 2007; Koo & Mckee 1992a,b). The structure of the interaction of a strong wind with the interstellar medium is described by the four zones: (1) freely expanding wind; (2) shocked stellar wind; (3) a shell of shocked interstellar gas; and (4) ambient gas (Weaver et al. 1977). The expanding molecular bubble surrounding Tycho has an inner radius $R_{\rm b} \sim 3\ d_{2.5}$ pc and an expansion velocity $V_{\rm b} \sim 4.5$ km s^{-1}. In the adiabatic condition, if the wind lasts until the SN explosion (e.g, see Fig. 1e in Han & Podsiadlowski 2004), the radius of the bubble (corresponding to the outer boundary of the shocked wind) is $R_{\rm b} = 0.66(\dot{M} v_{\rm w}^2/\rho_0)^{1/5} t_{\rm w}^{3/5}$, where $\rho_0 = 1.4 n_0 m_{\rm H}$ is the mass density of the ambient gas, with n_0 the number density of H atoms (Weaver et al. 1977). The duration of the wind is $t_{\rm w} = (3/5) R_{\rm b}/V_{\rm b} \sim 3.9 \times 10^5\ d_{2.5}$ yr. The density $n_0 \sim 18\ d_{2.5}^{-1}$ cm^{-3} is estimated from the mass, 220 $d_{2.5}^2\ M_\odot$, of the swept-up molecular gas surrounding the progenitor of Tycho. We estimate the wind velocity as $v_{\rm w} \sim 250\ (\dot{M}/3 \times 10^{-7} M_\odot\,{\rm yr}^{-1})^{-1/2}\ d_{2.5}^{1/2}$ km s^{-1} (see evolutionary path A in Table 2 for the case with $\dot{M} = 3 \times 10^{-7} M_\odot\,{\rm yr}^{-1}$). Here we constrain the wind velocity to be $\gtrsim 250$ km s^{-1} so that the modeled bubble is in the energy conservation stage. In this stage, the density of adiabatic gas in the shocked wind has a flat density profile (see Eq. 16 in Weaver et al. 1977), which could be consistent with the suggestion that the SNR is evolving in a uniform medium (Badenes et al. 2007; Yamaguchi et al. 2014). Since the mass-loss rates and durations of the wind vary in different outflow models (Han & Podsiadlowski 2004), if the wind stops long before the SN explosion, the observed $R_{\rm b}$ and $V_{\rm b}$ values can give multiple solutions of wind parameters [7]. Some exemplified evolutionary paths of the bubble are shown in Figure 4 with the parameters listed in Table 2, where a typical $\dot{M}$ value of $10^{-6}\,M_\odot\,{\rm yr}^{-1}$ is adopted. The gas density at the center of the shocked wind region is given by Castor et al. (1975) $n_b = 0.01\ (n_0/1\ {\rm cm}^{-3})^{19/35} (\dot{M}/10^{-6}\,M_\odot\,{\rm yr}^{-1})^{6/35} (v_{\rm w}/2000\,{\rm km\,s}^{-1})^{12/35} (t_{\rm w}/10^6\ {\rm yr})^{-22/35}$ cm^{-3}, which is further scaled as $n_b(t_b) \sim n_b(t_t)(R_t/R_{\rm b})^3$ if the elapse time $t_{elapse} = t_b - t_t$ between the wind stop and SN explosion cannot be ignored. The density estimates, $n_b(t_b) \sim 0.02$–$0.04\,{\rm cm}^{-3}$, for the interior of the bubble are consistent with the previous constraints for the SNR preshock gas obtained from X-ray ($\lesssim 0.2$ cm^{-3}; Katsuda et al. 2010) and infrared measurements (~ 0.03–0.5 cm^{-3}, Williams et al. 2013; the observed elevated density in the northeast can be related to the denser gas near the cavity wall). All of the wind parameters $v_{\rm w}$, $t_{\rm w}(t_t)$ and $\dot{M}$ match those expected in the SD scenario. There is also some observational evidence to support the existence of recurrent novae in outbursts before the SN explosion (Hachisu & Kato 2001), which may be an alternative outflow source to affect the circumstellar medium of the SNR.

TABLE 2
PARAMETERS FOR THE EXEMPLIFIED EVOLUTIONARY PATHS OF THE BUBBLE.

Path	$v_{\rm w}$ (km s^{-1})	$\dot{M}$ ($10^{-6} M_\odot$ yr^{-1})	t_t (10^5 yr)	t_{elapse} (10^5 yr)	$n_{\rm b}(t_t)$ (cm^{-3})	$n_{\rm b}(t_{\rm b})$ (cm^{-3})
A	250	0.3	3.9	0	0.04	0.04
B	250	1.0	1.3	1.6	0.09	0.02
C	280	1.0	1.1	1.7	0.10	0.03
D	350	1.0	0.8	1.8	0.13	0.02

A WBB will reach a maximum size $R_{\rm m}$ when it becomes in pressure equilibrium with the ambient medium: $R_{\rm m} = [(1/2) M_{\rm w} v_{\rm w}^2/(2\pi p)]^{1/3}$, where $M_{\rm w}$ is the total mass-loss of the wind (Chevalier 1999). For this expanding bubble, we have $R_{\rm m} > R_{\rm b} = 3 d_{2.5}$ pc, and hence we set a constraint on the mean wind velocity: $v_{\rm w} > 120 (M_{\rm w}/0.5\ M_\odot)^{-1/2} p_5^{1/2}\ d_{2.5}^{3/2}$ km s^{-1}. Our results support the theoretical predictions of a strong wind (over 100 km s^{-1}) driven by the SD progenitor system.

An earlier wind from the post-AGB star in the planetary nebula phase is unlikely to explain the current molecular bubble. Assuming that the bubble is created by an ejection of mass ($\sim 1\ M_\odot$ at a velocity of

[7] If the wind terminates at t_t (when the bubble size was R_t and velocity was V_t) prior to the SN explosion, we assume the bubble will continue to expand driven by the thermal pressure (p) of the shocked wind region. From the mass equation $dM = 4\pi R_b^2 \rho_0 dR_b$ and the momentum equation $d(MV_{\rm b}) = 4\pi R_{\rm b}^2 p$, the bubble radius is govern by $dR_{\rm b}/dt = \sqrt{V_t^2 R_t^6 + 2a_0(R_{\rm b} - R_t)}/R_{\rm b}^3$, where $a_0 = 3E_0 R_t^2/(2\pi\rho_0)$ with $E_0 = (5/11)\dot{M} v_{\rm w}^2 t_t/2$ (Weaver et al. 1977).

$\sim 10^3$ km s^{-1} for planetary nebulae) before the formation of a WD, the slowly expanding molecular bubble should have been in the radiative evolution phase with an age (Chevalier 1974): $0.3R_{\rm b}/V_{\rm b} \sim 2\times10^5$ yr, which is much smaller than the duration of the later evolution of either SD ($\sim 10^6$ yr; Hachisu et al. 1996) or DD progenitor systems ($> 10^6$ yr; Kashi & Soker 2011).

The disk wind and the later mass transfer should not last longer than the lifetime of the MCs (of the order of 10 Myr; see Mac Low & Klessen 2004 and references therein), or the molecular bubble would have vanished. Actually, the time between the onset of the wind and the SN explosion is less than a few Myr according to various SD models (see Badenes et al. 2007 and references therein). Compared with the core-collapse SNe, SNe Ia have much longer delay time (elapsed time between the formation of the star and the explosion SN; > 40 Myr; Maoz et al. 2011). The MC surrounding Tycho was probably newly formed in the vicinity of the progenitor binary, rather than the natal cloud.

5. SUMMARY

We have performed a ^{12}CO J=2–1 mapping and a 3-mm line survey toward the Type Ia SNR Tycho using the IRAM 30 m telescope. The main results are summarized as follows:

1. SNR Tycho appears to be confined in the clumpy ($< 11''$) molecular gas at $V_{\rm LSR} \sim -64$ to -60 km s^{-1}. In this velocity range, we have found a large ^{12}CO J=2–1-to-J=1–0 ratio (~ 1.6) and large ^{12}CO to^{13}CO ratios at the northeast of the remnant, where the shell is deformed and decelerated. These features provide kinematic evidence for the interaction between Tycho and the molecular gas.

2. We discover the expanding motion (~ 4.5 km s^{-1}) of the molecular bubble at $V_{\rm LSR} = -61$ km s^{-1}. The mass of the molecular bubble is $\sim 220\ d_{2.5}^2 M_\odot$ and the mean column density is $\sim 1.6\times10^{20}$ cm^{-2}. The SNR has been expanding in the low-density WBB and the shock wave has just reached the molecular cavity wall.

3. The most plausible origin for the expanding bubble is the fast outflow (with velocity hundreds of km s^{-1}) driven from the vicinity of the progenitor WD as it accreted matter from a nondegenerate companion star. The shocked wind confined in the molecular bubble has a uniform density ($\sim$ 0.02-0.04 cm^{-3}).

4. The MC surrounding Tycho was probably newly formed in the vicinity of the progenitor binary, rather than the natal cloud.

5. This is the first unambiguous detection of the expanding bubble driven by the progenitor of the Type Ia SNR, which provides important and independent evidence to support that the progenitor of Tycho was an SD system.

P.Z. is thankful to Dr. Fang-Jun Lu, Dr. Zhi-Yuan Li, and Prof. Noam Soker for helpful discussions and comments. P.Z. and Y.C. thank the support of NSFC grants 11503008, 11233001 and 11590781, the 973 Program grant 2015CB857100, and grant 20120091110048 by the Educational Ministry of China. Z.Z. acknowledges support from the European Research Council (ERC) in the form of an Advanced Grant, COSMICISM. X.L. was supported by NSFC under grant numbers 11133001 and 11333004. S.S.H. acknowledges support from the Canada Research Chairs program, the NSERC Discovery Grants program, and the Canadian Space Agency.

REFERENCES

Albinson, J. S., Tuffs, R. J., Swinbank, E., & Gull, S. F. 1986, MNRAS, 219, 427
Baade, W. 1945, ApJ, 102, 309
Badenes, C., Borkowski, K. J., Hughes, J. P., Hwang, U., & Bravo, E. 2006, ApJ, 645, 1373
Badenes, C., Hughes, J. P., Bravo, E., & Langer, N. 2007, ApJ, 662, 472
Blitz, L. 1993, Protostars and Planets III, 125
Bolatto, A. D., Wolfire, M., & Leroy, A. K. 2013, ARA&A, 51, 207
Broersen, S., Chiotellis, A., Vink, J., & Bamba, A. 2014, MNRAS, 441, 3040
Cai, Z.-Y., Yang, J., & Lu, D.-R. 2009, Chinese Astron. Astrophys. , 33, 393
Castor, J., McCray, R., & Weaver, R. 1975, ApJ, 200, L107
Chen, Y., Zhou, P., & Chu, Y.-H. 2013, ApJ, 769, L16
Chen, Y., Jiang, B., Zhou, P., et al. 2014, Supernova Environmental Impacts, 296, 170
Chevalier, R. A. 1974, ApJ, 188, 501
Chevalier, R. A. 1999, ApJ, 511, 798
Dame, T. M., Hartmann, D., & Thaddeus, P. 2001, ApJ, 547, 792
Dickman, R. L. 1978, ApJS, 37, 407
Gooch, R. 1996, Astronomical Data Analysis Software and Systems V, 101, 80
Hachisu, I., Kato, M., & Nomoto, K. 1996, ApJ, 470, L97
Hachisu, I., Kato, M., Nomoto, K., & Umeda, H. 1999, ApJ, 519, 314
Hachisu, I., & Kato, M. 2001, ApJ, 558, 323
Han, Z., & Podsiadlowski, P. 2004, MNRAS, 350, 1301
Hayato, A., Yamaguchi, H., Tamagawa, T., et al. 2010, ApJ, 725, 894
Ihara, Y., Ozaki, J., Doi, M., et al. 2007, PASJ, 59, 811
Jiang, B., Chen, Y., Wang, J., et al. 2010, ApJ, 712, 1147
Kashi, A., & Soker, N. 2011, MNRAS, 417, 1466
Kato, M., & Hachisu, I. 1999, ApJ, 513, L41
Katsuda, S., Petre, R., Hughes, J. P., et al. 2010, ApJ, 709, 1387
Kerzendorf, W. E., Yong, D., Schmidt, B. P., et al. 2013, ApJ, 774, 99
Koo, B.-C., & McKee, C. F. 1992a, ApJ, 388, 93
Koo, B.-C., & McKee, C. F. 1992b, ApJ, 388, 103
Krause, O., Tanaka, M., Usuda, T., et al. 2008, Nature, 456, 617
Krumholz, M. R., McKee, C. F., & Tumlinson, J. 2009, ApJ, 699, 850
Lee, J.-J., Koo, B.-C., & Tatematsu, K. 2004, Journal of Korean Astronomical Society, 37, 223
Li, X.-D., & van den Heuvel, E. P. J. 1997, A&A, 322, L9
Lu, F. J., Wang, Q. D., Ge, M. Y., et al. 2011, ApJ, 732, 11
Mac Low, M.-M., & Klessen, R. S. 2004, Reviews of Modern Physics, 76, 125
Maoz, D., Mannucci, F., Li, W., et al. 2011, MNRAS, 412, 1508
Perlmutter, S., Aldering, G., Goldhaber, G., et al. 1999, ApJ, 517, 565
Reynoso, E. M., Moffett, D. A., Goss, W. M., et al. 1997, ApJ, 491, 816
Reynoso, E. M., Velázquez, P. F., Dubner, G. M., & Goss, W. M. 1999, AJ, 117, 1827
Riess, A. G., Filippenko, A. V., Challis, P., et al. 1998, AJ, 116, 1009
Ruiz-Lapuente, P. 2004, ApJ, 612, 357

Schwarz, U. J., Goss, W. M., Kalberla, P. M., & Benaglia, P. 1995, A&A, 299, 193
Seta, M., Hasegawa, T., Dame, T. M., et al. 1998, ApJ, 505, 286
Tian, W. W., & Leahy, D. A. 2011, ApJ, 729, L15
Vink, J., Kaastra, J. S., & Bleeker, J. A. M. 1997, A&A, 328, 628
Warren, J. S., Hughes, J. P., Badenes, C., et al. 2005, ApJ, 634, 376
Weaver, R., McCray, R., Castor, J., Shapiro, P., & Moore, R. 1977, ApJ, 218, 377
Webbink, R. F. 1984, ApJ, 277, 355
Whelan, J., & Iben, I., Jr. 1973, ApJ, 186, 1007
Williams, B. J., Borkowski, K. J., Ghavamian, P., et al. 2013, ApJ, 770, 129
Xu, J.-L., Wang, J.-J., & Miller, M. 2011, Research in Astronomy and Astrophysics, 11, 537
Xue, Z., & Schaefer, B. E. 2015, ApJ, 809, 183
Yamaguchi, H., Badenes, C., Petre, R., et al. 2014, ApJ, 785, L27
Zhang, X., Chen, Y., Li, H., & Zhou, X. 2013, MNRAS, 429, L25